0026-895X/06/6903-1024–1032$20.00
MOLECULAR PHARMACOLOGY
Copyright © 2006 The American Society for Pharmacology and Experimental Therapeutics
Mol Pharmacol 69:1024–1032, 2006

Vol. 69, No. 3
18556/3090140
Printed in U.S.A.

Zinc and Mercuric Ions Distinguish TRESK from the Other Two-Pore-Domain K^+ Channels

Gábor Czirják and Péter Enyedi

Department of Physiology, Semmelweis University, Budapest, Hungary

Received August 31, 2005; accepted December 13, 2005

ABSTRACT

TWIK-related spinal cord K^+ channel (TRESK) is the most recently cloned two-pore-domain potassium ($2PK^+$) channel, regulated by the calcium/calmodulin-dependent protein phosphatase calcineurin. Functional identification of endogenous TRESK and its distinction from the other $2PK^+$ channels, producing similar background K^+ current, are impeded by the lack of specific inhibitors. Therefore, we searched for antagonists selective against TRESK among the mouse $2PK^+$ channels by screening more than 200 substances. Mibefradil, zinc, and mercuric ions inhibited TRESK expressed in *Xenopus laevis* oocytes with IC_{50} values lower than 10 μM. The specificity of the identified agents was determined by measuring their effects on mouse TALK-1, TASK-1, TASK-2, TASK-3, THIK-1, TRAAK, TREK-1, and TREK-2. Mibefradil failed to discriminate well among the functional $2PK^+$ channels; however, Zn^{2+} and Hg^{2+} exerted a significantly stronger inhibitory effect on TRESK than on the other channels. Sensitivity to zinc but insensitivity to ruthenium red were distinctive features of TRESK. Whereas both Zn^{2+} and Hg^{2+} were selective blockers of TRESK among the mouse $2PK^+$ channels, human TRESK was resistant to Zn^{2+}; it was blocked only by Hg^{2+}. His132 of mouse TRESK was partly responsible for this difference. Mouse TRESK expressed in COS-7 cells was also inhibited by Zn^{2+} and Hg^{2+}, and TRESK single-channel current was diminished in outside-out patches, indicating that the action of the ions was membrane-delimited, most probably targeting the channel itself. Thus, both Zn^{2+} and Hg^{2+} are expected to inhibit endogenous TRESK in isolated mouse cells, and these ions can be applied to identify the calcineurin-activated $2PK^+$ channel in its natural environment.

The high resting potassium conductance of the plasma membrane is established by background (leak) K^+ channels in several excitable and nonexcitable cell types. These background channels belong to the family of two-pore-domain K^+ ($2PK^+$) channels, and their regulation by distinct physicochemical parameters and intracellular signaling mechanisms has been reported to contribute essentially to cell function (Goldstein et al., 2001; Bayliss et al., 2003). Their widespread expression and functional importance urge the more detailed investigation of background K^+ currents in other cell types; however, the routine electrophysiological identification of two-pore-domain K^+ channels is still considerably impeded by the lack of specific inhibitors.

The mammalian $2PK^+$ channel family consists of 15 subunits divided into 6 subfamilies: TWIK, TASK, TREK, TALK, THIK, and TRESK. Dimers of these subunits constitute the functional channels. In most cases, this means homodimer formation, and heterodimerization has been reported only for one particular subunit combination (TASK-1/TASK-3) (Czirják and Enyedi, 2002). Members of the distinct subfamilies have strikingly different regulatory properties, but in general, standard whole-cell patch-clamp recording does not allow their unequivocal identification. Although the different $2PK^+$ channels exert a similar stabilizing effect on the resting membrane potential, it is obviously of central importance for the cell, whether this effect is achieved by pH-sensitive TASK (Talley et al., 2000), mechanosensitive TREK (Maingret et al., 2000), calcineurin-activated K^+ channel (TRESK) (Czirják et al., 2004), or by some other $2PK^+$ channels that have their own particular way of regulation.

We have reported that ruthenium red inhibited TASK-3 (and TRAAK, a member of TREK subfamily), but not TASK-1. This observation provided the essential pharmacological tool to demonstrate TASK-1/TASK-3 heteromerization (Czirják and Enyedi, 2002). Since that time, ruthenium red has been applied to examine the distribution of TASK

This work was supported by the Hungarian National Research Fund (OTKA T46954) and the Hungarian Medical Research Council (ETT-085/2003). G.C. was supported by the János Bolyai fellowship of the Hungarian Academy of Sciences.

Article, publication date, and citation information can be found at http://molpharm.aspetjournals.org.

doi:10.1124/mol.105.018556.

ABBREVIATIONS: $2PK^+$ channel, two-pore-domain K^+ channel; RR, ruthenium red; ANOVA, analysis of variance; HEK, human embryonic kidney; PCR, polymerase chain reaction; RT-PCR, reverse transcription-polymerase chain reaction; TRESK, TWIK-related spinal cord K^+ channel; HSD, honestly significant difference; EC, effective concentration; m, mouse; h, human.

subfamily members and their heteromerization in native cells (Lauritzen et al., 2003; Berg et al., 2004; Kang et al., 2004a; Larkman and Perkins, 2005). Despite of the overall nonselectivity of ruthenium red (e.g., it inhibits voltage-dependent calcium channels and the mitochondrial calcium uniporter), this compound turned out to be a valuable tool in the investigation of $2PK^+$ channels.

In the present study, we describe the aimed search for TRESK inhibitors. Our primary goal was to find substances selective for TRESK among the mouse $2PK^+$ channels and not necessarily presenting overall selectivity. These inhibitors may modify several other ion transport mechanisms in addition to TRESK, and thus care must be taken when they are applied in complex functional studies. However, because of their specificity within the $2PK^+$ channel family, they should be suitable for the analysis of the composition of background K^+ currents and consequently for the identification of TRESK in cells expressing the channel endogenously.

Endogenous TRESK mRNA expression was reported in the human spinal cord (Sano et al., 2003; Liu et al., 2004). We cloned TRESK also from mouse (AY325301) and demonstrated its mRNA to be expressed in cerebrum, cerebellum, brain stem, spinal cord, and testicular tissue by RT-PCR (Czirják et al., 2004). Mouse TRESK (with identical sequence, NM207261) was cloned simultaneously by another group (Kang et al., 2004b) and was named TRESK-2. In that study, high expression of TRESK was detected in rat thymus and spleen by Northern blot. Although human and mouse TRESK channels show low similarity (67%) at the amino acid level, the sequence of human TRESK-2 or mouse TRESK-1 has not been reported (and has not been found by us in the human or mouse genome, respectively). Therefore, in the present study, we use our original names: human TRESK (hTRESK) and mouse TRESK (mTRESK).

Human and mouse TRESK, expressed in *Xenopus laevis* oocytes, are regulated in a unique manner among the $2PK^+$ channels. The cytoplasmic calcium signal induces maintained (several minutes long) and strong (5- to 10-fold) stimulation of TRESK current through the activation of the Ca^{2+}/calmodulin-dependent protein phosphatase, calcineurin (Czirják et al., 2004). By this regulation, cells expressing TRESK are expected to respond with maintained hyperpolarization and reduction of excitability to a single cytoplasmic calcium signal. The capability to store the memory of a foregoing calcium signal renders TRESK particularly interesting, and the identification of endogenous TRESK may facilitate further studies and shed light on the functional role of calcium-mediated background K^+ current regulation in different cell types. With the present work, we open up the way for these investigations by demonstrating that mouse TRESK can be discriminated from the other $2PK^+$ channels based on its high sensitivity to zinc and mercuric ions.

Materials and Methods

Materials. Enzymes and kits for molecular biological studies were purchased from Ambion (Austin TX), Amersham (Little Chalfont, Buckinghamshire, UK), Fermentas (Vilnius, Lithuania), New England Biolabs (Beverly, MA), Pharmacia Biotech (Uppsala, Sweden), Promega (Madison, WI), QIAGEN (Valencia, CA), and Stratagene (La Jolla, CA). Fine chemicals of analytical grade were obtained from Fluka (Buchs, Switzerland), Promega, and Sigma Chemical Co. (St. Louis, MO). The substances applied in the first round of screening were mixed (powder), dissolved in ethanol (0.2–0.4 M each), and further diluted with the high $[K^+]$ perifusing solution to 10 to 20 mM stock solutions. Mibefradil (30 mM) was dissolved in ethanol, ruthenium red (20 mM) in distilled water, mercuric chloride (30 mM) in high $[K^+]$ perifusing solution, and zinc chloride (30 mM) in 10 mM HCl to prevent the formation of zinc oxychloride precipitate. These stock solutions were diluted further to the desired concentration before the measurements were taken.

Cloning of Mouse $2PK^+$ Channels. Total RNA was isolated from mouse tissues with TRIzol reagent (Invitrogen, Paisley, UK) according to the manufacturer's instructions. The RNA was denatured (70°C, 4 min) in the presence of random hexanucleotides (Promega) and reverse-transcribed by Moloney murine leukemia virus-reverse transcriptase (Fermentas) at 37°C for 40 min, followed with 42°C for 20 min. TASK-1, TASK-3, and TWIK-2 coding regions were amplified by the high-fidelity Pfu Turbo polymerase (Stratagene); TALK-1 was amplified by HotStar Taq (QIAGEN); TASK-2, THIK-1, and TREK-2 were amplified by five cycles with HotStar Taq followed by a 10-fold dilution and 31 cycles with Pfu Turbo. In the TASK-3 Pfu reaction, 2% dimethyl sulfoxide was included for promoting denaturation. Denaturing temperatures for Pfu and HotStar Taq reactions were 98 and 94°C (30–60 s in the cycles), and the initial denaturations lasted 2 and 14 min, respectively. Annealing temperatures, numbers of cycles, and primer sequences are given in Table 1 for each reaction. In some cases, the touchdown PCR methodology was applied, and the annealing temperature was decreased in every three cycles at the beginning of the reaction. Extensions were per-

TABLE 1

Oligonucleotide sequences, annealing temperatures, and restriction enzyme sites for PCR and cloning of mouse $2PK^+$ channels

Forward (top) and reverse (bottom) primers are shown for each channel. The incorporated restriction enzyme sites are marked with lowercase letters. The third column contains the annealing temperatures and the number of cycles performed at the given temperature during the PCR amplification.

Channel	Oligonucleotide (5′→3′)	°C:Cycles	Restriction Enzyme
mTALK-1	CAGgaattcGCCACCATGCCCCGTGCTGGGGTCTG	55:36	EcoRI-XhoI
	GCGctcgagTCATGCAGAGATGGGGATTTTC		
mTASK-1	CAGgaattcGGAGGGACGATGAAGCGGCAG	72:3, 69:3, 66:3, 62:27	EcoRI-XhoI
	GGTGctcgagGTCTGGCTGTGGTTC		
mTASK-2	GCGcaattgTCCAGAGTCATGGTGGACCG	55:36	MunI-XhoI
	GCGctcgagTCACGTGCCCCTGGGGTTATC		
mTASK-3	CAGgaattcGCGGCCATGAAGCGGCAG	65:3, 62:3, 59:3, 57:27	EcoRI-SalI
	ATACCgtcgacTTAGATGGACTTGCGACGGAG		
mTHIK-1	CAGgaattcTCCAGTGCCATGGCTGGCCG	55:36	EcoRI-XhoI
	GCGctcgagGTTCCTACCTATCTCCACTGGTC		
mTREK-2	GCGcaattgATCCCCCTGTGGGCAACGGAG	55:36	MunI-SalI
	ATACCgtcgacTTTAAGGCACGTGTCTCAGTGTG		
mTWIK-2	CAGgaattcACGGGCACCATGCGGCGGGG	72:3, 69:3, 66:3, 62:27	EcoRI-XhoI
	GCGctcgagGTCGACAGCTACCTGGGGATG		

formed at 72°C for 110 to 140 s in the cycles, and there was a 5-min final extension at the end of the reaction.

Taking advantage of the EcoRI and XhoI compatible restriction enzyme sites incorporated into the 5′ end of the forward and reverse primers (Table 1), respectively, the PCR products were cleaved and cloned between the EcoRI and XhoI sites of pEXO vector. Thus, the complete coding sequences of the mouse channels were positioned between the 5′ and 3′ untranslated regions of the *X. laevis* globin gene, present in pEXO, to increase the stability of the cRNA transcripts in *X. laevis* oocytes. The fidelity of our clones was verified by automatic sequencing and comparison to published, genomic, and expressed sequence tag data. No mutation was generated during the PCR reactions.

In Vitro Site-Directed Mutagenesis of Mouse TRESK. In vitro site-directed mutagenesis was performed according to the manufacturer's instructions using the QuikChange site-directed mutagenesis kit (Stratagene). Complementary primer pairs were designed, coding for the desired mutation together with discriminating silent mutations (introducing new restriction enzyme sites). The sense primer sequences are listed in Table 2. The mutant clones were identified by restriction enzyme mapping and automatic sequencing.

Synthesis of Ion Channel cRNA. All channel coding regions [including the newly amplified mouse $2PK^+$ channels, our formerly published mTRESK and hTRESK (Czirják et al., 2004) and those kindly provided by others] were cloned or subcloned to pEXO. These DNA templates were linearized at the XbaI site of the vector and purified with QIAGEN PCR Purification Kit. The cRNAs coding for the channels were synthesized in vitro using the Ambion mMESSAGE mMACHINE T7 in vitro transcription kit, according to the manufacturer's instructions.

Animals and Tissue Preparation and *X. laevis* Oocyte Injection. Oocytes were prepared as described previously (Czirják and Enyedi, 2003). The cells were injected 1 day after defolliculation. Fifty nanoliters of the appropriate cRNA solution was delivered with Nanoliter Injector (World Precision Instruments, Saratosa, FL). Electrophysiological experiments were performed 3 or 4 days after the injection. All treatments of the animals were conducted in accordance with state laws, institutional regulations, and National Institutes of Health guidelines. The experiments were approved by the Animal Care and Ethics Committee of the Semmelweis University.

Electrophysiological Recordings. Membrane currents of whole oocytes were recorded by two-electrode voltage clamp (Warner Instrument Corporation, Hamden, CT) using microelectrodes made of thin-walled borosilicate glass (Clark Electromedical Instruments, Pangbourne, UK) with resistance of 0.3 to 1 MΩ when filled with 3 M KCl. Currents were filtered at 1 kHz and digitally sampled at 1 to 2.5 kHz. Low $[K^+]$ solution contained 95.4 mM NaCl, 2 mM KCl, 1.8 mM $CaCl_2$, and 5 mM HEPES, pH 7.5 with NaOH. High $[K^+]$ perifusing solution contained 80 mM K^+ (78 mM Na^+ of the low $[K^+]$ solution was replaced with K^+). Background K^+ currents were measured in high EC $[K^+]$ at the end of 300-ms long voltage steps to −100 mV applied every 3 s. The holding potential was 0 mV. For estimating the amplitude of the background current, the inward current in high $[K^+]$ was corrected for the small nonspecific leak measured in 2 mM EC $[K^+]$ at −100 mV.

Currents of *X. laevis* outside-out membrane patches were recorded with Axopatch 1D amplifier (Axon Instruments, Foster City, CA) using microelectrodes made of thick-walled borosilicate glass (Clark Electromedical Instruments) with a resistance of 30 to 80 MΩ when coated with R-6101 elastomer (Dow Corning, Midland, MI), fire-polished, and filled with pipette solution containing 140 mM KCl, 2 mM $MgCl_2$, 5 mM EGTA, and 10 mM HEPES, pH 7.3 with NaOH. Bath solution contained 140 mM KCl, 1 mM $CaCl_2$, 4 mM $MgCl_2$, and 10 mM HEPES, pH 7.4 with NaOH. Oocytes were devitellinized manually in a hyperosmotic solution containing 200 mM DL-aspartic acid, 20 mM KCl, 1 mM $MgCl_2$, 5 mM EGTA, and 10 mM HEPES, pH 7.4 with KOH. For low-noise recordings, seal resistance was greater than 20 GΩ. Cut-off frequency of the eight-pole Bessel filter was adjusted to 2 kHz, data were acquired at 10 kHz, and the recordings were not filtered further. The charge carrier of the single-channel events recorded at −90 mV was verified to be K^+ in all examined patches by transiently substituting 136 mM K^+ with Na^+ in the bath solution (data not shown).

Membrane currents of COS-7 cells were recorded with RK-400 amplifier (Biologic, Claix, France) using microelectrodes made of thin-walled borosilicate glass (Clark Electromedical Instruments) with a resistance of 3 to 9 MΩ when fire-polished and filled with the same pipette solution as used for single-channel recording. Low (4 mM) and high (140 mM) $[K^+]$ bath solutions also had the same composition as those used for *X. laevis* membrane patches.

All experiments were carried out at room temperature, and solutions were applied by gravity-driven perfusion systems. Recordings were digitally sampled by Digidata Interface 1200 (Axon Instruments). Recording and data analysis were performed using pCLAMP software 6.0.4 (Axon Instruments).

Statistics and Calculations. Data are expressed as means ± S.E.M. Normalized dose-response curves were fitted by least-squares method (Origin 6.0; OriginLab Corp., Northampton, MA) to Hill equation of the form $y = 1/(1 + (c/K_{1/2})^n)$, where c is the concentration, $K_{1/2}$ is the concentration at which half-maximal inhibition occurs, and n is the Hill coefficient. If the inhibition was not complete, a modified form of the Hill equation was used: $y = \alpha/(1 + (c/K_{1/2})^n) + (1 - \alpha)$, where α is the fraction inhibited by the treatment. Zero segments were detected, and the average current of single-channel traces was calculated by a computer program developed in our laboratory. Statistical significance was estimated by the nonparametric Mann-Whitney U test and one- or two-way ANOVA followed by Tukey honest significant difference (HSD) test for post hoc pairwise comparisons (Statistica 6.0 program package; Statsoft, Tulsa, OK), and the difference was considered to be significant at $p < 0.05$.

Results

Mibefradil, Zinc, and Mercuric Ions Inhibit Mouse TRESK, Expressed in *X. laevis* Oocytes at Micromolar Concentrations. The effect of the inhibitors on the inward background K^+ current was measured by the two-electrode voltage-clamp technique in high (80 mM) extracellular $[K^+]$ at −100 mV in *X. laevis* oocytes expressing mouse TRESK. Inhibitors of mouse TRESK were searched by screening the

TABLE 2

Oligonucleotide sequences and incorporated restriction enzyme sites for in vitro site-directed mutagenesis of mouse and human TRESK

The sense primer sequences are shown for each mutation. The nucleotides changed for altering the amino acid sequence are underlined. Mutations contributing to the new restriction enzyme sites are marked with lowercase letters.

Mutation	Sense Oligonucleotide (5′→3′)	Restriction Enzyme
C77,82S	CCTGGACGATCTGTcgAACATCCTGAAATcgAACCTGACAGTGGTTG	TaqI
C95S	GTAGCAGGAAGAACTTaaGTGAGCATCTGCAAC	Tru1I
C121,122S	CTCTCTTCTTCTCgTcgACAGTGTTCAGCAC	SalI
C329S	GGATGCTTTCTACTTCAGCTTTGTGACtCTGACCACCATCG	HinfI
H132Y, M133I	CAGTGGGTTATGGCTACATCTACCCgGTCACCAGGCTCGG	Eco91I
Y121H, I122M	ACCGTGGGCTATGGCcAtATgTACCCCGTCACCAGG	NdeI

substances available in our laboratory. In the first round of screening, 24 mixtures, each containing 10 different substances at 5 to 10 μM concentrations, were tested. In the second round, constituents of the three mixtures, yielding the highest inhibitions in the first round, were examined separately. From these 30 substances, mibefradil, zinc, and mercuric ions emerged as the effective agents.

Next, the dose-response relationships of our three identified channel blockers were determined. Mibefradil inhibited mouse TRESK with an IC_{50} of 2.2 μM (Fig. 1, A and B), whereas the inhibition by zinc had a slightly higher IC_{50} value of 5.3 μM (Fig. 1, D and E). The effects of mibefradil and zinc were characterized by Hill coefficients of 0.75 and 0.78, respectively, suggesting that one inhibitor molecule/ion bound to one TRESK channel. For both substances, the inhibition appeared instantaneously, and it was readily reversible (Fig. 1, C and F). In contrast, mercuric ion inhibited mTRESK slowly, and the kinetics of inhibition depended apparently on the concentration of the ion (Fig. 2A). The effect of Hg^{2+} was detectable even at a concentration as low as 100 nM; however, steady-state inhibition by this concentration was not established in 2.5 min. Therefore, the exact IC_{50} value for Hg^{2+} has not been determined, but it is apparent in Fig. 2A that the value must be smaller than 1 μM. Recovery from mercuric inhibition was very slow (Fig. 2B), and thus the inhibition may be regarded irreversible in most applications.

Zinc and Mercuric Ions Discriminate TRESK from the Other Mouse $2PK^+$ Channels, but Mibefradil Fails to Distinguish It Well. For determining whether a background K^+ current is constituted by TRESK, an inhibitor specific for TRESK within the $2PK^+$ channel family is suitable. Therefore, the effects of our TRESK inhibitors were examined on the known functional mouse $2PK^+$ channels. Mouse TRAAK and TREK-1 were already available in our laboratory. The sequence of mouse TALK-1, TASK-1, TASK-2, and THIK-1 were published and/or deposited to GenBank (National Center for Biotechnology Information, Bethesda, MD) previously (BD170722, NM010608, NM021542, and NM_146037, respectively), and these channels were cloned by RT-PCR from pancreas, cerebellum, kidney, and testis RNA, respectively, based on this information. The cloning of TASK-3, TREK-2, and TWIK-2 has not been reported from mouse; thus, the sequences of the murine homologs of these channels were determined by comparing the published sequences with the mouse genomic and expressed sequence tag databases (National Center for Biotechnology Information GenBank). The newly derived sequences were also amplified by RT-PCR (TASK-3 and TREK-2 from cerebellum, TWIK-2 from kidney RNA), cloned, and expressed in *X. laevis* oocytes. The new mouse $2PK^+$ channel sequences were deposited to GenBank under the accession numbers TASK-3 (DQ185133), TREK-2 (DQ185134), and TWIK-2 (DQ185135).

After measuring the effect of mibefradil (3 μM) on five further $2PK^+$ channel types (some members of the TASK and TREK subfamilies, see Fig. 3A), it became clear that the drug inhibited all of them, and the extent of the inhibition was not remarkably different from one channel to the other. Especially the inhibition of TASK-1 (47 $\pm$ 2%) was close to the value characteristic for TRESK (60 $\pm$ 1%). Thus, mibefradil cannot be applied as a specific TRESK inhibitor within the $2PK^+$ channel family.

Mouse TRESK was inhibited more strongly (65 $\pm$ 3%) by zinc (10 μM) than were the other $2PK^+$ channels ($p < 0.001$, Tukey HSD test for all mTRESK versus other channel comparisons, Fig. 3B). Human TRESK was not influenced under identical conditions (2 $\pm$ 2% inhibition), suggesting that the sensitivity to low concentrations of zinc is not a general property of TRESK but depends on the examined species. Most of the other mouse $2PK^+$ channels were slightly activated by Zn^{2+} or were not influenced at all. Apart from TRESK, only TASK-3 and TRAAK were inhibited by the ion; however, the inhibition was weak (13 $\pm$ 2 and 11 $\pm$ 2%, respectively). Because it has been reported (Czirják and Enyedi, 2002) that both TASK-3 and TRAAK are sensitive to ruthenium red (RR), we also examined the effect of Zn^{2+} on TRESK in the presence of RR. High (10 μM) concentration of RR induced maximal block of TASK-3 and TRAAK but caused only negligible TRESK inhibition (15 $\pm$ 2%, Fig. 4, A–C). In the presence of RR, zinc failed to inhibit TASK-3 and

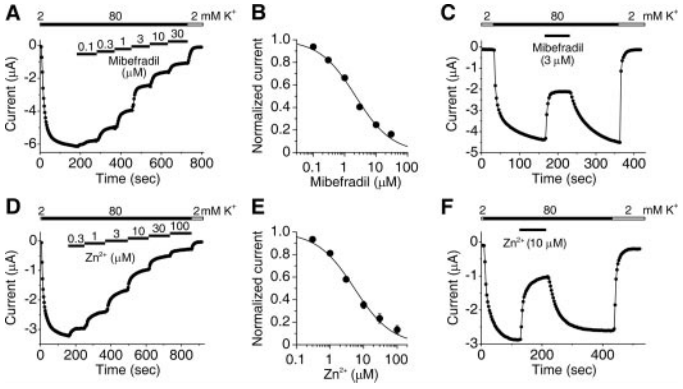

Fig. 1. Concentration-dependent inhibition of mouse TRESK by mibefradil and zinc. A and D, representative currents of *X. laevis* oocytes expressing mTRESK are shown in extracellular solutions of different K^+ and mibefradil (A) or zinc (D) concentrations (as indicated above the curves). The plotted inward currents were measured at the end of 300-ms long voltage steps to -100 mV applied every 3 s from a holding potential of 0 mV. B and E, mibefradil (B) and zinc (E) dose-response relationships. Inhibition was measured as shown in A and D. The currents were corrected for the small nonspecific leak in 2 mM extracellular $[K^+]$ at -100 mV and normalized to the value without the inhibitors. Each data point represents the average of normalized currents of five to seven oocytes. Error bars are smaller than symbols in most cases. The data points were fitted by Hill equation (see *Materials and Methods*). C and F, representative recordings demonstrating reversibility of the inhibition by mibefradil (C) and zinc (F). The method of measurement was the same as in A and D.

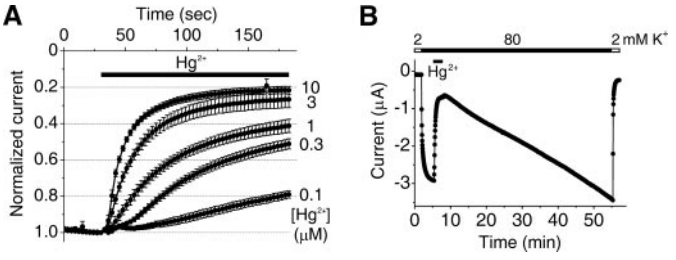

Fig. 2. Concentration- and time-dependent inhibition of mouse TRESK by mercuric ion. A, TRESK current expressed in *X. laevis* oocytes was inhibited by different concentrations of mercuric ion, as indicated on the right side. The current was measured in 80 mM EC $[K^+]$ at -100 mV. Each trace represents the average current of five oocytes, normalized to the value before the application of Hg^{2+}. B, slow recovery of mTRESK current was evoked by extensive washout after a brief exposure to Hg^{2+} (10 μM). Note the long time scale of the recording.

TRAAK further (1% inhibition and 2% activation, respectively, expressed in the percentage of the original current), but the extent of the additional TRESK inhibition (55%) induced by the administration of zinc in the presence of RR was similar to that measured in the absence of RR (Fig. 4D). Thus, zinc is even more selective for TRESK in the presence of ruthenium red. Sensitivity to zinc after the elimination of TASK-3 and TRAAK currents by ruthenium red is a distinctive feature of TRESK among the mouse $2PK^+$ channels.

TRESK was by far the most strongly inhibited $2PK^+$ channel by mercuric ion (72 ± 4 and 78 ± 2% inhibition for the human and mouse channel, respectively, by 3 μM Hg^{2+}, $p < 0.03$, Tukey HSD test for all mTRESK or hTRESK versus other channel comparisons; Fig. 3C). THIK-1 was the only other inhibited $2PK^+$ channel; however, its inhibition was much weaker (13 ± 2%) than that of TRESK. Some members of the TASK and TREK subfamilies (TASK-3, TREK-1, and TREK-2) were activated by more than 50% by 3 μM Hg^{2+}. This activation may mask TRESK inhibition if one of these channels was coexpressed with TRESK in a comparable quantity. However, the pattern of mercuric inhibition of mouse $2PK^+$ channels unequivocally suggests that the strong reduction of a background K^+ current of unknown composition by mercuric ion is a predicting indicator of the significant contribution of TRESK to that examined current.

Inhibition of Mouse TRESK by Zinc and Mercuric Ions in Mammalian COS-7 Cells Is Voltage-Independent. Cytosolic and membrane composition of the oocyte of amphibian *X. laevis* may differ in many aspects from those of mammalian cells. To exclude the possibility that the mechanism of action of our inhibitors relied on oocyte-specific components, we also expressed mouse TRESK in the mammalian COS-7 cell line and measured its sensitivity to Zn^{2+} and Hg^{2+} with the whole-cell patch-clamp technique. In this experiment, the degree of voltage-dependence of the inhibition was estimated by a slow-ramp protocol in identical 140 mM extra- and intracellular [K^+]. Under these conditions, the background TRESK current was a nearly linear function of the voltage with a reversal potential at 0 mV (Fig. 5). Application of both Zn^{2+} and Hg^{2+} simply transformed this current-voltage relationship to a less steep line, indicating that the inhibition was not voltage-dependent (Fig. 5, B and D). The extent of inhibition [51 ± 4% for Zn^{2+} (10 μM, $n = 5$) and

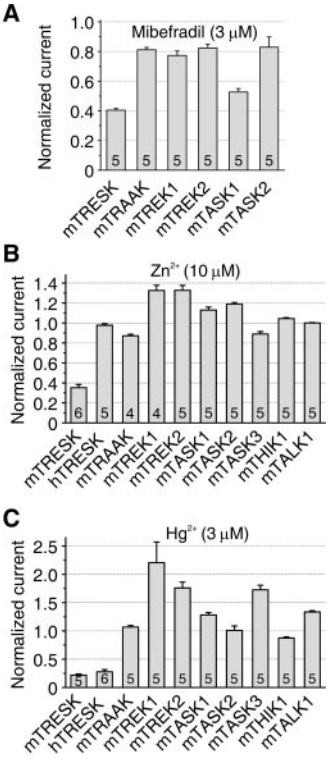

Fig. 3. Sensitivity of $2PK^+$ channels to mibefradil, zinc, and mercuric ions. Mouse $2PK^+$ channels and human TRESK were expressed in *X. laevis* oocytes, and their sensitivity to the given inhibitor (shown above the columns) was measured and calculated as in Fig. 1. The numbers in the columns indicate the number of the examined oocytes. Data for mTRESK are repeated from Figs. 1 and 2.

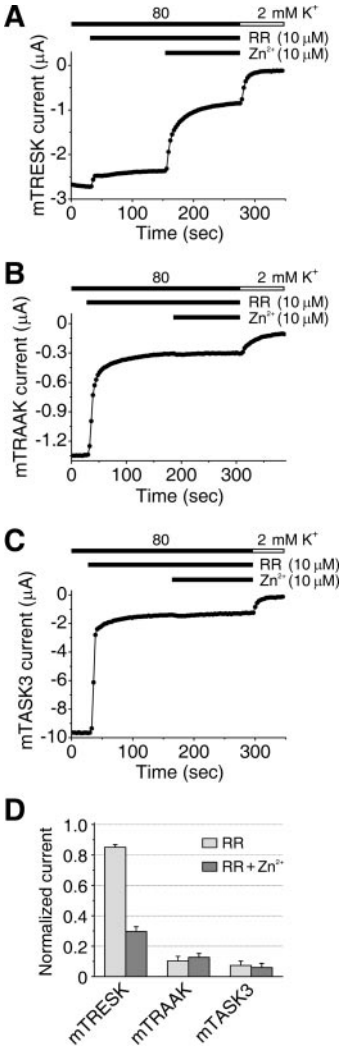

Fig. 4. Among the zinc-sensitive mouse $2PK^+$ channels, TRESK is the only one resistant to ruthenium red. A to C, representative currents of three oocytes expressing mTRESK, mTRAAK, and mTASK-3, respectively, were measured with the same voltage protocol as in Fig. 1A. In 80 mM EC [K^+], the currents were inhibited first by ruthenium red (10 μM) and subsequently by zinc in the continued presence of ruthenium red (10 μM for both inhibitors), as indicated by the horizontal bars above the curves. At the end of the measurements, the small nonspecific leak was estimated by changing the EC [K^+] to 2 mM. D, the currents, inhibited to steady state by ruthenium red (light columns) or ruthenium red plus zinc (dark columns), were normalized to the current measured before the addition of the inhibitors. For each channel, the average of four to five oocytes is depicted.

88 ± 1% for Hg^{2+} (3 μM, $n = 5$)] was similar to that obtained in *X. laevis* oocytes.

Zinc and Mercuric Ions Inhibit TRESK Also at the Single Channel Level in Excised, Outside-Out Membrane Patches. To prove that the effect of Hg^{2+} and Zn^{2+} is membrane-delimited and does not depend on an intracellular indirect mechanism, the inhibitors were also tested in a cell-free system, outside-out membrane patches of *X. laevis* oocytes. These patches contained only a few mTRESK channels, and the composition of the solution on both sides of the membrane was controlled experimentally, excluding the possibility of the interaction of cytosolic regulators. The inward current of a single active mTRESK channel at −90 mV in symmetrical 140 mM [K^+] is characterized by trains of short (typically <2 ms) spike-like openings (Fig. 6, inset), and consequently the flickery currents of a few channels are summed up to an irregular control curve of higher amplitude (Fig. 6, A. and C, top curves). Because this type of activity does not allow the estimation of the probability of opening and unitary current separately, instead of these parameters, we calculated the average current from the curves. Both Hg^{2+} (3 μM) and Zn^{2+} (30 μM) reduced the average single-channel current (see Fig. 6, A and C, for representative traces, and B and D for statistical analysis). This indicates that the action of Hg^{2+} and Zn^{2+} is membrane-delimited, and the most probable target of the ions is the TRESK channel itself.

Mutation of Extracellular Cysteine Residues at Positions 77 and 82 to Serines Significantly Decreases the Inhibition by Mercuric Ion. Because Hg^{2+} inhibits many target proteins by binding to the SH groups of cysteine residues, we mutated all extracellular cysteines of mouse TRESK to serines one by one, or in pairs, in which the residues were close to each other. Some of these mutations reduced severely the K^+ current obtained by expressing the channel in *X. laevis* oocytes. When Cys329 was mutated to serine in the second extracellular loop, no K^+ current could be measured. TRESK C77,82S double mutant produced 0.6 ± 0.1 μA ($n = 6$) background K^+ current when its cRNA was microinjected at 25-fold higher concentration than that of the wild type (inducing 2.6 ± 0.3 μA in the same oocyte preparation, $n = 7$). Nevertheless, the expression of C121,122S, C77,82S, and C95S mutants (first extracellular loop) allowed the measurement of their Hg^{2+} sensitivity (Fig. 7). Whereas the sensitivity of the C121,122S and C95S mutants was not significantly different from the wild type, the C77,82S mutant was much less inhibited (43 ± 6% inhibition) than the wild type (76 ± 3% inhibition). Therefore, cysteine 77 and 82 may contribute to the Hg^{2+} binding site of mouse TRESK.

H132Y,M133I Double Mutation Decreases mTRESK Sensitivity to Zinc, whereas Y121H,I122M Double Mutation of hTRESK Enhances the Inhibition by the Ion. Zinc was suggested to interact with His98 residue located directly after the GYG K^+ channel signature sequence in the first pore domain of TASK-3 (Clarke et al., 2004). Because mouse TRESK contains histidine after its GYG but human TRESK has a tyrosine, it was feasible to assume that this may contribute to the different zinc sensitivity of mouse and human TRESK channels. It has been reported recently that mutating the histidine to tyrosine in mTRESK or mutating the tyrosine to histidine in hTRESK resulted in nonfunctional subunits (Keshavaprasad et al., 2005). Because the

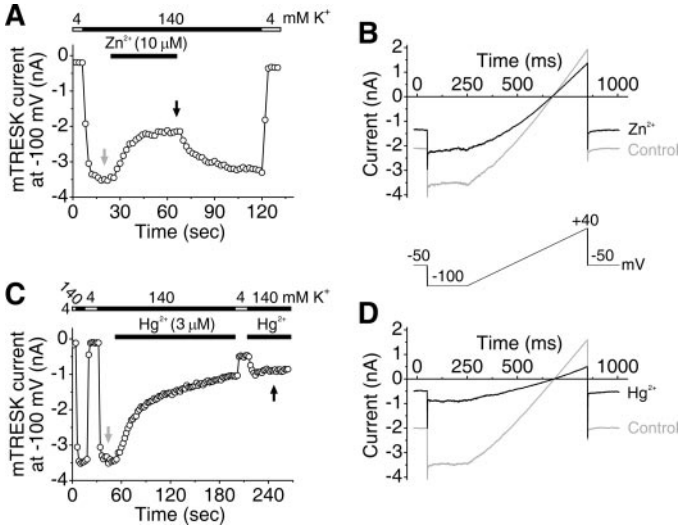

Fig. 5. Zinc and mercuric ions inhibit mouse TRESK voltage-independently in COS-7 cells. A and C, representative currents of COS-7 cells expressing TRESK are shown during the application of zinc (A) or mercuric ions (C), as indicated by the horizontal bars above the curves. The plotted values were sampled at the end of the voltage steps to −100 mV applied in every 2 s (see the inset between B and D for the voltage protocol). The EC 140 mM [K^+] was reduced occasionally to 4 mM (as indicated above the curves) for estimating TRESK K^+ current. B and D, current traces evoked by the voltage ramp protocol in the absence (gray) and presence of the inhibitor (black) was plotted. These current traces correspond to the episodes marked with gray and black vertical arrows in A and C.

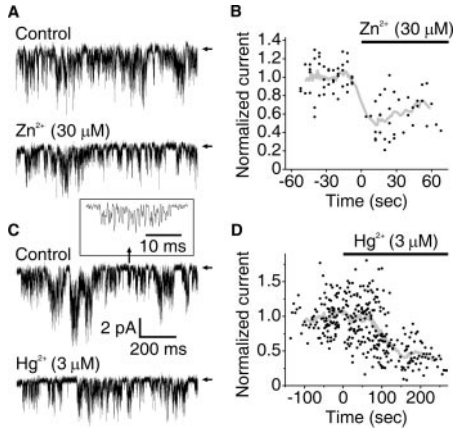

Fig. 6. Zinc and mercuric ions reduce TRESK single-channel current in outside-out membrane patches of *X. laevis* oocytes. A and C, mouse TRESK single-channel activity was detected at −90 mV in symmetrical 140 mM EC and IC [K^+] in the absence (top curve) and in the presence (bottom curve) of Zn^{2+} (A) or Hg^{2+} (C). Note the reduced area between the curve and the zero level and the higher proportion of zero segments in the presence of the inhibitors. Zero current levels are indicated by horizontal arrows. The scale bars in C apply to both panels. In the framed inset, representing the TRESK single-channel event marked with a vertical arrow, only the time scale was extended. B and D, every data point in these plots represents the average of a 950-ms long current trace (similar to those illustrated in A and C). These current traces were recorded every 4 s before and after the addition of the inhibitors. The inhibitors were administered at 0 s, as indicated by the horizontal black bars. All data points were normalized to the average of the data points measured before the addition of the inhibitor in the same membrane patch; thus, the values of the control period scatter around 1. The thick gray curves are constituted by straight lines connecting the moving averages of every seven (Zn^{2+}) or 21 (Hg^{2+}) neighboring data points. Data points around 0 s were omitted because of the solution-changing artifact. Both ions inhibited mTRESK significantly ($p < 10^{-6}$, Mann-Whitney U test; in the case of Hg^{2+}, the data points measured after 150 s were compared with those of the control period).

pore domain sequence of mTRESK (FSTVGYGHMYPVTRL) differs from that of hTRESK (FSTVGYGYIYPVTRL) only in two amino acids in this region, we hypothesized that both residues have to be interchanged to obtain functional channels. Indeed, both of the mTRESK double mutants containing YI instead of HM and the hTRESK double mutant containing HM instead of YI were functional in *X. laevis* oocytes. Inhibition of the double mutant mTRESK by Zn^{2+} was deteriorated (IC_{50} value increased to 157 from 5.3 μM, characteristic for the wild type; Fig. 8A), whereas the double mutant hTRESK became slightly sensitive to Zn^{2+} (Fig. 8B). The remaining inhibition of the double mutant mTRESK and the limited efficacy and potency of Zn^{2+} toward the double mutant human channel suggest that other residues may also be involved in the constitution of the zinc binding site; however, our results clearly indicate that the pore vicinal histidine plays a pivotal role in the determination of zinc sensitivity.

Discussion

Mibefradil, zinc, and mercuric ions have been applied extensively in the investigation of ion channel functions. Mibefradil was originally described as a selective inhibitor of the low voltage-activated T-type calcium channels (Mishra and Hermsmeyer, 1994). A wide range of IC_{50} values (approximately 0.1–3 μM) was reported in different studies because the potency of mibefradil for T channels was highly dependent on the examined preparations, and even in the case of cloned calcium channels, it was strongly influenced by the experimental conditions (Martin et al., 2000). In certain cell types, the drug was not selective enough to distinguish between T- and the high voltage-activated L-type calcium channels, and potassium conductances were also modified by the same (or even lower) drug concentration (Liu et al., 1999).

For the most part, the delayed and inward-rectifier K^+ channels were highly sensitive to mibefradil (Chouabe et al., 1998; Gomora et al., 1999; Perchenet and Clement-Chomienne, 2000). Mibefradil has also been described to inhibit the background K^+ current of bovine adrenal zona fasciculata cells and its equivalent $2PK^+$ channel, bovine TREK-1 expressed in HEK-293 cells, with an IC_{50} value of 0.5 μM (Enyeart et al., 2002). In our experiment, mouse TREK-1 was less sensitive to the drug (23% inhibition by 3 μM). This may reflect a species difference; however, the amino acid sequences of bovine and mouse TREK-1 are 97% identical. On the other hand, TREK-1 inhibition by mibefradil may be strongly dependent on the experimental conditions, similarly to the case of the T-type calcium channel.

Mibefradil was identified as a potent inhibitor of mouse TRESK by our screening procedure. Although TRESK was blocked most potently, mibefradil inhibited all $2PK^+$ channels examined in this study, and the slight differences of the inhibitions indicated that mibefradil cannot be used as a selective TRESK inhibitor. Therefore, in addition to delayed and inward rectifiers, mibefradil is a nonspecific inhibitor of $2PK^+$ channels too. Our results reinforce the view that besides T-type voltage-gated calcium channels, modification of several potassium conductances (including those of $2PK^+$ channels) may have contributed to the side effects of this drug, formerly used as an antihypertensive medicine.

Whereas mercuric ion is an insidious environmental pollutant, zinc is an important trace element, essential for life, and is incorporated in the active site of many enzymes. Therefore, zinc-specific transporters have evolved, and the distribution of Zn^{2+} is regulated by these proteins (Liuzzi and Cousins, 2004). One example for zinc compartmentalization is the sequestration of the ion in zinc-containing neurons (Takeda, 2000). In response to depolarization, zinc is released from the synaptic vesicles of these specialized glutamatergic neurons, and its concentration is estimated to reach levels between 10 and 100 μM in the synaptic cleft (Vogt et al., 2000; Li et al., 2001). This concentration may modulate several ion conductances, and it has been recently suggested that some $2PK^+$ channels are also possible targets of the synaptically released zinc. Human TASK-3 was inhibited by zinc with IC_{50} values of 12.7 and 19.8 μM in HEK-293 cells and *X. laevis* oocytes, respectively (Clarke et al., 2004; Gruss et al., 2004). In turn, TREK-2 was activated by zinc in *X. laevis* oocytes with an EC_{50} value of 87.1 μM, and this activation was suggested to be a specific hallmark of TREK-2 among the $2PK^+$ channels (Kim et al., 2005).

In this study, we performed the systematic analysis of zinc sensitivity of functional mouse $2PK^+$ channels. From the 15 cloned mammalian $2PK^+$ channel subunits, 12 form functional plasma membrane channels in *X. laevis* oocytes. It has

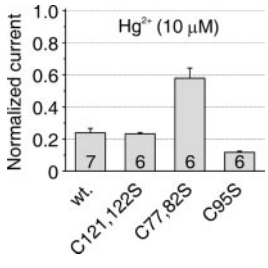

Fig. 7. Mutation of cysteines 77 and 82 of mouse TRESK to serines reduces mercuric inhibition. Wild-type and mutant mTRESK channels, in which different extracellular cysteines were replaced by serines, were expressed in *X. laevis* oocytes, and their sensitivity to Hg^{2+} (10 μM) was measured as in Fig. 1. The numbers in the columns indicate the number of the examined oocytes. Inhibition of the C77,82S double mutant was significantly weaker than that of the wild-type channel ($p < 0.001$, Tukey HSD post hoc comparison after one-way ANOVA).

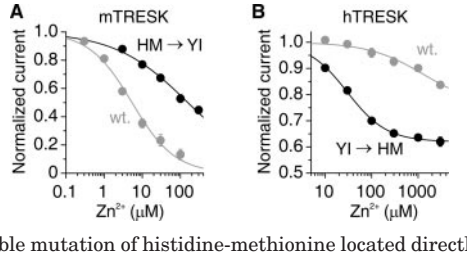

Fig. 8. Double mutation of histidine-methionine located directly after the GYG K^+ channel signature sequence in the first pore domain to tyrosine-isoleucine reduces the Zn^{2+} sensitivity of mouse TRESK, whereas double mutation of tyrosine-isoleucine to histidine-methionine in the corresponding position of the human channel engenders Zn^{2+} sensitivity. A, zinc dose-response relationship of H132Y,M133I double mutant mTRESK (black) was measured as in Fig. 1. For comparison, the dose-response relationship of the wild type (wt.) mouse channel (gray) was repeated from Fig. 1E. B, zinc dose-response relationships of the wild-type (gray) and Y121H,I122M double mutant (black) hTRESK channels were plotted. Data points represent the average of normalized currents of five to nine oocytes, and the error bars are smaller than symbols in most cases. The data points were fitted by Hill equation (A) or a modified Hill equation (see *Materials and Methods*) for incomplete inhibition (B). Dose-response relationships of the wild-type and mutant channels were significantly different for both human and mouse TRESK ($p < 10^{-6}$, two-way ANOVA).

been reported that KCNK7 (a member of the TWIK family) (Salinas et al., 1999), TASK-5 (Kim and Gnatenco, 2001), and THIK-2 (Rajan et al., 2001) cannot be functionally expressed. Although in some studies, small TWIK-1 and TWIK-2 currents were measured after high overexpression (Lesage et al., 1996; Chavez et al., 1999), it has been described recently that a specific mechanism targets the vast majority of TWIK-1 channels to recycling endosomes (Decressac et al., 2004). Therefore, the dominant location of members of the TWIK family may be intracellular. Similarly to previous observations (Goldstein et al., 1998; Pountney et al., 1999), we did not obtain currents by expressing the original mouse TWIK-1 (Lesage et al., 1997) or our sequence-verified mouse TWIK-2 clone in *X. laevis* oocytes. Mouse TALK-2 has not been cloned, because its genomic sequence was incomplete in GenBank. Zinc sensitivity of the remaining nine functional mouse $2PK^+$ channels was tested.

Our results are in accordance with the published data in the sense that TASK-3 was slightly inhibited and TREK-2 was slightly activated by 10 μM Zn^{2+}. However, TREK-1 was also activated identically in *X. laevis* oocytes, indicating that the two closely related TREK channels share the property of activation by zinc. Thus, our data do not support the conclusion of Kim et al. (2005), that activation by zinc is specific for TREK-2 among the $2PK^+$ channels. Furthermore, considering the zinc resistance of human TREK-1 in HEK-293 cells (Gruss et al., 2004), it seems that the activation of TREK-1 by Zn^{2+} depends on the examined species or the applied expression system.

Zinc inhibited mouse TRESK with IC_{50} values of 5.3 and 10 μM in *X. laevis* oocytes and in COS-7 cells, respectively. Although these values are smaller than those published previously for any of the $2PK^+$ channels, they are close to the IC_{50} values of TASK-3. Moreover, in addition to TRESK and TASK-3, we detected a slight inhibition of one further $2PK^+$ channel, TRAAK, by zinc. These results indicate that by using zinc alone, these three channel types cannot be discriminated efficiently. However, as a lucky coincidence, TASK-3 and TRAAK channels were reported to be highly sensitive to ruthenium red (Czirják and Enyedi, 2002). We also demonstrated formerly that glutamate 70 residues of both TASK-3 subunits of the homodimer were required for the binding of a single RR molecule (Czirják and Enyedi, 2003). Later, the importance of the same TASK-3 residues in the binding of zinc was emphasized (Clarke et al., 2004). The inhibitory mechanism of TRAAK is different from that of TASK-3, because the effect of RR on TRAAK is characterized by a Hill coefficient of 2.1 (Czirják and Enyedi, 2002), suggesting the involvement of multiple (most probably two) binding sites on the TRAAK homodimer. It remains unknown whether RR and Zn^{2+} interact with the same amino acid side chains in TRAAK. Whereas TASK-3 and TRAAK were blocked by both RR and Zn^{2+}, TRESK was only negligibly influenced by high concentrations of RR. Therefore, the zinc binding site of TRESK does not bind RR, and consequently, inhibition by zinc in the presence of ruthenium red is diagnostic for TRESK among the $2PK^+$ channels.

Mercuric ion has been used as an inhibitor of water channels known as aquaporins (Gunnarson et al., 2004). Hg^{2+} inhibits aquaporins by binding to certain cysteine residues (Preston et al., 1993), and as an SH reagent, it also modifies dozens of other enzymatic reactions and transport mechanisms. To our knowledge, the effect of Hg^{2+} on $2PK^+$ channels has not been investigated so far. Herein, we report that the mercuric ion is a potent inhibitor of both mouse and human TRESK, whereas it activates mouse TASK-3, TREK-1, and TREK-2 markedly. Localization of the Zn^{2+} and Hg^{2+} binding sites on the external face of TRESK was strongly supported by the effect of the ions in outside-out membrane patches. The voltage-independent inhibition by these inorganic blockers indicated that the sites of interaction are outside of the transmembrane electrical field. The pore vicinal His132 was identified as a major contributor to the zinc binding site of mouse TRESK. This is similar to the voltage-independent inhibition of TASK-3 by Zn^{2+}, in which His98 was reported to be involved in the inhibitory mechanism in addition to glutamate 70 (Clarke et al., 2004). The slowly developing and practically irreversible inhibition by Hg^{2+} suggested that this ion acted as an SH reagent. Replacing each extracellular cysteine with serine (its closest structural analog) resulted in two mutant channels significantly different from the wild type. Whereas the C329S mutant was not functional, the C77,82S double mutant expressed a smaller current that was less sensitive to Hg^{2+}. Therefore, these residues are likely constituents of the Hg^{2+} binding site.

High sensitivity of TRESK, TASK-3, TREK-1, and TREK-2 to Hg^{2+} and their expression in the central nervous system suggest that the modulation of these $2PK^+$ channels may contribute to the ataxia, visual and auditory deficits, and other neurotoxic effects of mercuric ion. Whereas Hg^{2+} may bind to $2PK^+$ channels in vivo only in the case of poisoning, binding of zinc may also happen physiologically, as suggested for TASK-3 previously (Clarke et al., 2004; Gruss et al., 2004). Nevertheless, it is intriguing that the zinc sensitivity of TRESK does not seem to be evolutionary conserved, or at any rate, there is a tremendous difference in the affinities between mice and humans. Whether we will learn in the future that zinc regulates TRESK physiologically or not, it can be stated unambiguously that zinc and mercuric ions are valuable pharmacological tools for the identification of TRESK in electrophysiological experiments.

Acknowledgments

We thank Professor M. Lazdunski and Dr. F. Lesage for pEXO, pEXO-mTRAAK, pEXO-mTREK-1, and pBS-mTWIK plasmids. The expert technical assistance of Irén Veres and Beáta Busi is highly appreciated.

References

Bayliss DA, Sirois JE, and Talley EM (2003) The TASK family: two-pore domain background K^+ channels. *Mol Intervent* **3:**205–219.

Berg AP, Talley EM, Manger JP, and Bayliss DA (2004) Motoneurons express heteromeric TWIK-related acid-sensitive K^+ (TASK) channels containing TASK-1 (KCNK3) and TASK-3 (KCNK9) subunits. *J Neurosci* **24:**6693–6702.

Chavez RA, Gray AT, Zhao BB, Kindler CH, Mazurek MJ, Mehta Y, Forsayeth JR, and Yost CS (1999) TWIK-2, a new weak inward rectifying member of the tandem pore domain potassium channel family. *J Biol Chem* **274:**7887–7892.

Chouabe C, Drici MD, Romey G, Barhanin J, and Lazdunski M (1998) HERG and KvLQT1/IsK, the cardiac K^+ channels involved in long QT syndromes, are targets for calcium channel blockers. *Mol Pharmacol* **54:**695–703.

Clarke CE, Veale EL, Green PJ, Meadows HJ, and Mathie A (2004) Selective block of the human 2-P domain potassium channel, TASK-3 and the native leak potassium current, IKSO, by zinc. *J Physiol* **560:**51–62.

Czirják G and Enyedi P (2002) Formation of functional heterodimers between the TASK-1 and TASK-3 two-pore domain potassium channel subunits. *J Biol Chem* **277:**5426–5432.

Czirják G and Enyedi P (2003) Ruthenium red inhibits TASK-3 potassium channel by interconnecting glutamate 70 of the two subunits. *Mol Pharmacol* **63:**646–652.

Czirják G, Tóth ZE, and Enyedi P (2004) The two-pore domain K^+ channel, TRESK,

is activated by the cytoplasmic calcium signal through calcineurin. *J Biol Chem* **279:**18550–18558.
Decressac S, Franco M, Bendahhou S, Warth R, Knauer S, Barhanin J, Lazdunski M, and Lesage F (2004) ARF6-dependent interaction of the TWIK1 K^+ channel with EFA6, a GDP/GTP exchange factor for ARF6. *EMBO (Eur Mol Biol Organ) Rep* **5:**1171–1175.
Enyeart JJ, Xu L, Danthi S, and Enyeart JA (2002) An ACTH- and ATP-regulated background K^+ channel in adrenocortical cells is TREK-1. *J Biol Chem* **277:** 49186–49199.
Goldstein SA, Bockenhauer D, O'Kelly I, and Zilberberg N (2001) Potassium leak channels and the KCNK family of two-P-domain subunits. *Nat Rev Neurosci* **2:**175–184.
Goldstein SA, Wang KW, Ilan N, and Pausch MH (1998) Sequence and function of the two p domain potassium channels: implications of an emerging superfamily. *J Mol Med* **76:**13–20.
Gomora JC, Enyeart JA, and Enyeart JJ (1999) Mibefradil potently blocks ATP-activated K^+ channels in adrenal cells. *Mol Pharmacol* **56:**1192–1197.
Gruss M, Mathie A, Lieb WR, and Franks NP (2004) The two-pore-domain K^+ channels TREK-1 and TASK-3 are differentially modulated by copper and zinc. *Mol Pharmacol* **66:**530–537.
Gunnarson E, Zelenina M, and Aperia A (2004) Regulation of brain aquaporins. *Neuroscience* **129:**947–955.
Kang D, Han J, Talley EM, Bayliss DA, and Kim D (2004a) Functional expression of TASK-1/TASK-3 heteromers in cerebellar granule cells. *J Physiol* **554:**64–77.
Kang D, Mariash E, and Kim D (2004b) Functional expression of TRESK-2, a new member of the tandem-pore K^+ channel family. *J Biol Chem* **279:**28063–28070.
Keshavaprasad B, Liu C, Au JD, Kindler CH, Cotten JF, and Yost CS (2005) Species-specific differences in response to anesthetics and other modulators by the K2P channel TRESK. *Anesth Analg* **101:**1042–1049.
Kim D and Gnatenco C (2001) TASK-5, a new member of the tandem-pore K^+ channel family. *Biochem Biophys Res Commun* **284:**923–930.
Kim JS, Park JY, Kang HW, Lee EJ, Bang H, and Lee JH (2005) Zinc activates TREK-2 potassium channel activity. *J Pharmacol Exp Ther* **314:**618–625.
Larkman PM and Perkins EM (2005) A TASK-like PH- and amine-sensitive 'Leak' K^+ conductance regulates neonatal rat facial motoneuron excitability in vitro. *Eur J Neurosci* **21:**679–691.
Lauritzen I, Zanzouri M, Honore E, Duprat F, Ehrengruber MU, Lazdunski M, and Patel AJ (2003) K^+-dependent cerebellar granule neuron apoptosis. Role of task leak K^+ channels. *J Biol Chem* **278:**32068–32076.
Lesage F, Guillemare E, Fink M, Duprat F, Lazdunski M, Romey G, and Barhanin J (1996) TWIK-1, a ubiquitous human weakly inward rectifying K^+ channel with a novel structure. *EMBO (Eur Mol Biol Organ) J* **15:**1004–1011.
Lesage F, Lauritzen I, Duprat F, Reyes R, Fink M, Heurteaux C, and Lazdunski M (1997) The structure, function and distribution of the mouse TWIK-1 K^+ channel. *FEBS Lett* **402:**28–32.
Li Y, Hough CJ, Suh SW, Sarvey JM, and Frederickson CJ (2001) Rapid translocation of Zn^{2+} from presynaptic terminals into postsynaptic hippocampal neurons after physiological stimulation. *J Neurophysiol* **86:**2597–2604.
Liu C, Au JD, Zou HL, Cotten JF, and Yost CS (2004) Potent activation of the human tandem pore domain K^+ channel TRESK with clinical concentrations of volatile anesthetics. *Anesth Analg* **99:**1715–1722.
Liu JH, Bijlenga P, Occhiodoro T, Fischer-Lougheed J, Bader CR, and Bernheim L (1999) Mibefradil (Ro 40-5967) inhibits several Ca^{2+} and K^+ currents in human fusion-competent myoblasts. *Br J Pharmacol* **126:**245–250.
Liuzzi JP and Cousins RJ (2004) Mammalian Zinc Transporters. *Annu Rev Nutr* **24:**151–172.
Maingret F, Lauritzen I, Patel AJ, Heurteaux C, Reyes R, Lesage F, Lazdunski M, and Honore E (2000) TREK-1 is a heat-activated background K^+ channel. *EMBO (Eur Mol Biol Organ) J* **19:**2483–2491.
Martin RL, Lee JH, Cribbs LL, Perez-Reyes E, and Hanck DA (2000) Mibefradil block of cloned T-type calcium channels. *J Pharmacol Exp Ther* **295:**302–308.
Mishra SK and Hermsmeyer K (1994) Selective inhibition of T-type Ca^{2+} channels by Ro 40–5967. *Circ Res* **75:**144–148.
Perchenet L and Clement-Chomienne O (2000) Characterization of mibefradil block of the human heart delayed rectifier HKv1.5. *J Pharmacol Exp Ther* **295:**771–778.
Pountney DJ, Gulkarov I, Vega-Saenz de ME, Holmes D, Saganich M, Rudy B, Artman M, and Coetzee WA (1999) Identification and cloning of TWIK-originated similarity sequence (TOSS): a novel human 2-pore K^+ channel principal subunit. *FEBS Lett* **450:**191–196.
Preston GM, Jung JS, Guggino WB, and Agre P (1993) The mercury-sensitive residue at cysteine 189 in the CHIP28 water channel. *J Biol Chem* **268:**17–20.
Rajan S, Wischmeyer E, Karschin C, Preisig-Muller R, Grzeschik KH, Daut J, Karschin A, and Derst C (2001) THIK-1 and THIK-2, a novel subfamily of tandem pore domain K^+ channels. *J Biol Chem* **276:**7302–7311.
Salinas M, Reyes R, Lesage F, Fosset M, Heurteaux C, Romey G, and Lazdunski M (1999) Cloning of a new mouse two-P domain channel subunit and a human homologue with a unique pore structure. *J Biol Chem* **274:**11751–11760.
Sano Y, Inamura K, Miyake A, Mochizuki S, Kitada C, Yokoi H, Nozawa K, Okada H, Matsushime H, and Furuichi K (2003) A novel two-pore domain K^+ channel, TRESK, is localized in the spinal cord. *J Biol Chem* **278:**27406–27412.
Takeda A (2000) Movement of zinc and its functional significance in the brain. *Brain Res Brain Res Rev* **34:**137–148.
Talley EM, Lei Q, Sirois JE, and Bayliss DA (2000) TASK-1, a two-pore domain K^+ channel, is modulated by multiple neurotransmitters in motoneurons. *Neuron* **25:**399–410.
Vogt K, Mellor J, Tong G, and Nicoll R (2000) The actions of synaptically released zinc at hippocampal mossy fiber synapses. *Neuron* **26:**187–196.

Address correspondence to: Dr. Péter Enyedi, Department of Physiology, Semmelweis University, P.O. Box 259, Budapest, Hungary, H-1444. E-mail: enyedi@puskin.sote.hu